Assembly and Disassembly of the Photosystem II Manganese Cluster Reversibly Alters the Coupling of the Reaction Center with the Light-Harvesting Phycobilisome†

Hong Jin Hwang, Aparna Nagarajan, Aaron McLain, and Robert L. Burnap*

Department of Microbiology and Molecular Genetics, Oklahoma State University, Stillwater, Oklahoma 74078

Received April 1, 2008; Revised Manuscript Received June 14, 2008

ABSTRACT: The light-driven oxidative assembly of Mn^{2+} ions into the H_2O oxidation complex (WOC) of the photosystem II (PSII) reaction center is termed photoactivation. The fluorescence yield characteristics of *Synechocystis* sp. PCC6803 cells undergoing photoactivation showed that basal fluorescence, F_0, exhibited a characteristic decline when red, but not blue, measuring light was employed. This result was traced to a progressive increase in the coupling of the phycobilisome (PBS) to the PSII reaction center as determined by observing the changes in room temperature and 77 K fluorescence emission spectra that accompany photoactivation. The results support the hypothesis that strong energetic coupling of the PBS to the PSII reaction center depends upon the formation of an active WOC, which presumably diminishes the likelihood of photodamage to reaction centers that have either lost an intact Mn cluster or are in the process of assembling an active WOC.

The assembly of Mn^{2+} ions to form the catalytically active Mn_4-Ca cluster of the water oxidation complex (WOC[1]) of the photosystem II (PSII) reaction center is a light-driven process termed photoactivation (reviewed in refs *1* and *2*). Photoactivation occurs during the *de novo* formation of PSII as well as during the frequent repair of PSII, which occurs in response to photoinhibition. During photoactivation, Mn^{2+} ions are oxidized to $Mn^{\geq 3+}$ as they become coordinated within the ligation environment provided by the D1 and CP43 proteins of the PSII complex (*3–6*). The same set of redox cofactors involved in charge separation in fully assembled PSII complex are also involved in the initial photooxidation events leading to the photoactivation of the WOC. Specifically, the oxidized forms of the primary and secondary donors, P_{680}^+ and $Y_Z^{\bullet}$, respectively, are involved in the oxidation of incoming Mn^{2+} ions during photoactivation. Additional PSII redox cofactors, not directly involved in water oxidation catalysis, such as cytochrome b_{559}, may have a role in protecting the PSII complex against photodamage prior to and during the assembly of the manganese cluster (*7–14*). The functioning of the additional redox cofactors is important because photoactivation is a low quantum efficiency process, unlike the relatively high quantum efficiency for the turnover of the assembled water oxidation enzyme. Typical overall quantum yields for photoactivation are in the range of 0.005 to 0.01 as opposed to near unity for the fully assembled reaction center charge separation and stabilization (*7, 15–18*). The precise reasons for this low quantum efficiency of photoactivation are still under investigation, but it is clear that this situation renders reaction centers in the process of photoactivation to be prone to photodamage. In the absence of a fully functional manganese cluster, secondary donors, including cytochrome b_{559} and a redox active β-carotene, may be required to quench the strong oxidizing power of P_{680}^+ to avoid destructive side reactions that might occur during episodes of sluggish donor-side electron transfer as may occur during photoactivation. Thus, the alternative secondary donors are important to minimize the frequency of photochemical damage that could otherwise occur with high quantum yield in the absence of a functional manganese cluster.

Besides alternative electron donors, the modulation of the optical cross section of PSII undergoing photoactivation could be important to minimize photodamage, although information in this area is lacking. Light intensity dependence measurements show that the rate of photoactivation saturates at very low light intensities compared the intensities required to saturate photosynthesis (*15, 17, 19–21*). The low light saturation of photoactivation is due to unique kinetic features that characterize the assembly mechanism. Kinetic analyses have indicated an obligatory sequence for the binding and photooxidation of the first two Mn^{2+} ions during their assembly into the apoprotein. Indeed, it appears that formation of the first properly bound Mn^{3+} species is the prerequisite to the binding of the subsequent Mn^{2+} ions. A refractory "dark-rearrangement" step ($t_{1/2}$ ~100 ms) occurs early in the assembly sequence, probably immediately after the photooxidation of the first Mn^{2+} incorporated. This light

† This work was supported by the National Science Foundation (MCB-0818371 to R.L.B.).

* Corresponding author. Phone: 405-744-7445. Fax: 405-744-6790. E-mail: rob.burnap@okstate.edu.

[1] Abbreviations: BMF, blue measuring flash; DCBQ, 2,6-dichlorobenzoquinone; EDTA, (ethylenedinitrilo)tetraacetic acid; HA, hydroxylamine (NH_2OH); Hepes, 4-(2-hydroxyethyl)-1-piperazineethanesulfonic acid; HBG-11, normal BG-11 growth medium buffered with Hepes-NaOH pH 8; PSII, photosystem II; PBS, phycobilisome; RMF, red measuring flash; WOC, H_2O oxidation complex of PSII; F_0', the fluorescence value immediately before the actinic flash in the photoactivating flash sequence.

10.1021/bi800568p CCC: $40.75
Published on Web 08/22/2008

independent refractory step remains poorly understood, but may reflect a molecular or charge rearrangement. Because this step is rate-limiting, the process of photoactivation is saturated at light intensities at least 10-fold lower than the intensities that saturate the operation of the overall photosynthetic mechanism. Consequently, reaction centers undergoing photoactivation during biogenesis or during the frequent PSII repair cycle cannot productively utilize the higher levels of excitation energy reception as compared to the assembled PSII complex. Therefore, a mechanism modulating the coupling of light harvesting to reaction centers in the process of photoactivation may be advantageous to avoid overexcitation and possible photodamage in nascent PSII. Here, we explore this hypothesis by examining the fluorescence properties of cyanobacterial cells undergoing the process of photoactivation.

MATERIALS AND METHODS

Strains and Growth Conditions. The glucose-tolerant strain of *Synechocystis* sp. PCC6803 was routinely maintained in BG-11 medium as described previously (*22*). The D1-D170A strain was a gift from Prof. Rick Debus and has been extensively characterized (*23–26*). Experimental cultures were propagated in BG-11 media buffered with 20 mM Hepes-NaOH, pH 8.0 (HBG-11) under a PFD (photon flux density) of 80 μmol m^{-2} s^{-1} at 30 °C. Cultures were bubbled with filter sterilized air that was enriched with 3% CO_2. Light intensity measurements were made with a LiCor sensor (Lincoln, NE).

Photoactivation of Hydroxylamine-Extracted Cells. Cells from cultures in late-log growth phase were harvested and extracted with hydroxylamine (HA) and photoactivated by exposure to saturating single turnover xenon flashes as described previously (*16, 27, 28*). At the completion of the photoactivation flash treatment, 100 μL aliquots were withdrawn for assay, either for determination of light-saturated rates of O_2 evolution or for measurements of fluorescence properties. Light-saturated rates of O_2 evolution were determined using a Clark-type electrode by resuspending in HN (10 mM Hepes, pH 7.2, 30 mM NaCl) buffer supplemented with an artificial electron acceptor system consisting of 0.8 mM DCBQ and 1 mM potassium ferricyanide, and oxygen evolution was measured in response to saturating orange (>570 nm) illumination at 30 °C. Fluorescence as a function of photoactivation treatment was performed as follows: 300 μL aliquots were resuspended with HBG-11 to a concentration of 5 μg of Chl mL^{-1}, incubated five to ten minutes in the dark prior to measuring fluorescence. Flash-induced fluorescence yield kinetics were measured by a FL3000 double modulation fluorometer (PSI Instruments, Brno) (*29, 30*) in the 50 μs to 100 s postactinic flash time range at a sample concentration of 5 μg of Chl mL^{-1}. For "real-time" photoactivation-fluorescence experiments, photoactivation was conducted directly in the fluorometer using saturating LED pulses with concurrent measurement of fluorescence. A series of 3000 saturating flashes in the form of 30 μs pulses from an array of red (617 and 625 nm) light-emitting diodes (LEDs) given at intervals of 0.5 s to the HA-extracted cells suspended in HBG-11 to 5 μg of Chl mL^{-1}. Extra illumination was provide by an auxiliary flash head to ensure saturation of cells due to the apparent uncoupling of phycobilisomes (PBS) due to HA-extraction as described below. Responses to the actinic flashes in fluorescence yields were obtained by application sequence of weak (roughly 5% of saturating) red measuring flashes (RMF) (617 nm), or alternatively blue measuring flashes BMF (455 nm).

Fluorescence Emission Spectra. Fluorescence spectra on samples were measured in a Jobin Yvon-Fluomax-3 fluorescence spectrophotometer. The slit sizes of excitation and emission were set at 5 and 2 nm, respectively. The 77 K fluorescence spectra were collected from 600 to 750 nm for two different excitations at 435 nm for exciting chlorophyll and 600 nm for exciting for phycobilins of the phycobilisome (PBS). Room temperature emission spectra were recorded from 620 to 750 nm of with excitation at 600 nm in an optical cuvette at a sample concentration of 5 μg of Chl mL^{-1}. Dark adapted samples at 5 μg of Chl mL^{-1} were applied as a thin coat on glass rods of radius of 5 mm cooling the rods in liquid nitrogen and briefly dipping the cooled rods into the sample solution and returned to liquid nitrogen where they were stored (~10 min) until acquisition of the emission spectra. For measurement, the coated glass rods were placed in a Dewar vessel filled with liquid nitrogen and positioned so that the glass rods could be manually turned about its lengthwise axis while retaining its position and orientation. To account for position-sensitive variation in fluorescence yield from the frozen samples, each sample glass rod was rotated incrementally and measured a total of 3 times to generate one averaged emission spectrum. At least three independent repeats of this procedure were used to generate the final emission spectrum for each sample.

RESULTS

The kinetics of room temperature chlorophyll fluorescence provides a useful probe of electron transfer events occurring in PSII and provides a measure of the development of functional PSII during the process of Mn_4-Ca assembly during photoactivation (*7, 31*). In the absence of a functional Mn_4-Ca cluster, fluorescence yield following actinic illumination is low compared with the maximal yields observed in the presence of a fully functional Mn_4-Ca. The reasons for the low fluorescence yield are complex, but are in large measure due to the relatively high concentration of fluorescence quencher, P_{680}^+, that accumulates in the absence of an efficient donor to oxidized Y_Z (*32, 33*). Photoactivation restores the Mn_4-Ca, allowing the efficient formation of the highly fluorescent P_{680}-Q_A^- state and maximal fluorescence. Figure 1 shows the fluorescence kinetics of *Synechocystis* cells extracted with hydroxylamine (HA) to remove PSII Mn and subjected to a sequence of saturating flashes with a xenon flash lamp to promote photoactivation. Samples at intermediate stages of photoactivation were withdrawn from the photoactivation mixture, dark adapted ~5 min, and analyzed in the absence (panel A) or presence (panel B) of DCMU, using a double modulated chlorophyll fluorometer (*29, 30*). The individual traces in these multitrace plots show the relaxation of fluorescence yield following a single saturating flash as measured using a succession of weak red probe flashes. As expected, the amplitude of fluorescence for each individual trace was minimal immediately prior to the flash (F_0), maximal (F_m) at the first measuring pulse 50 μs after

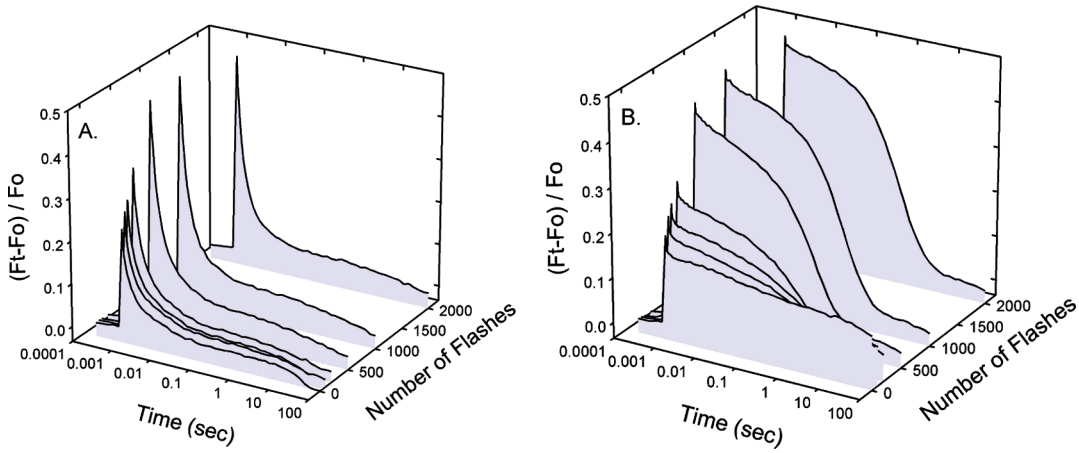

FIGURE 1: Induction and decay of Q_A^- in response of a saturating flash in HA-extracted cells at different stages of a photoactivation experiment. Sequences of photoactivating flashes were given with uniform interval of 0.5 s to HA-extracted cells in the absence (panel A) and presence (panel B) of DCMU. Cells were given a discrete number of saturating Xe flashes (*z*-axes), withdrawn from a reaction vessel, dark adapted 5 min, and given a single saturating 30 μs LED actinic flash, and changes in fluorescence yield were monitored with a train of weak red measuring flashes (RMF). Values of variable fluorescence yield are displayed according to the equation $(F_t - F_0)/F_0$, where F_t is the fluorescence yield recorded for each of the time points after the flash, starting 50 μs postactinic flash, and F_0 is the fluorescence yield recorded 10 μs before the flash. F_{max} is taken as the value of this equation computed using the 50 μs time point. These experiments were performed at least three times, and representative traces are shown.

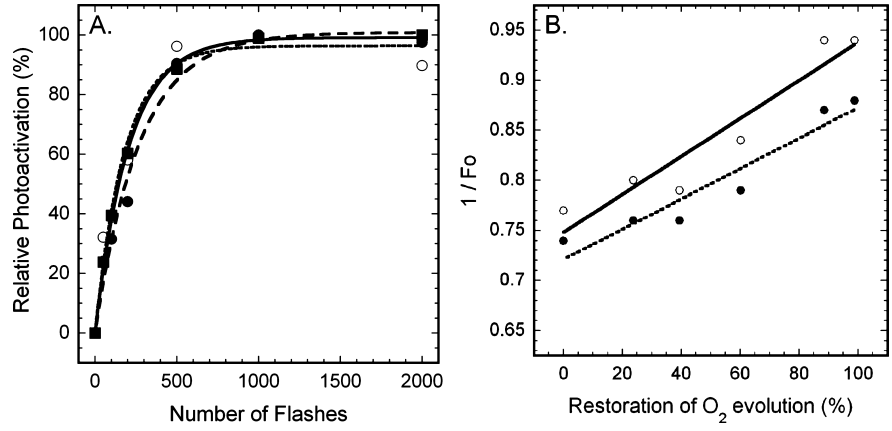

FIGURE 2: Relationship between photoactivation kinetics of oxygen evolution and fluorescence yield ($(F_m - F_0)/F_0$) during photoactivation. Panel A shows the development of oxygen evolution activity and a function of flash number (filled squares and solid line) and the development of the maximum fluorescence yield ($(F_m - F_0)/F_0$) measured in the absence (filled circles and dotted line) and presence (open circles and dashed line) of DCMU. For the latter, DCMU was added after application of photoactivation flashes. Data were fit assuming a monoexponential rise in the conversion of apo-PSII centers to active PSII. Panel B shows the relationship between the restoration of O_2-evolving activity and the inverse of the changes on F_0 based upon the data shown in panel A. The values of F_0 were determined in the absence (filled circles and dotted line) and presence (open circles and solid line) of DCMU added after application of photoactivation flashes.

the actinic flash, and decaying during the remainder of the postflash trace. With or without DCMU, the maximal fluorescence increased in proportion to number of flashes during photoactivation consistent with previous studies (*7, 31*).

The development of maximal variable fluorescence, calculated as $(F_m - F_0)/F_0$, closely matched with development of O_2 evolution during photoactivation by flash number (Figure 2A). During the course of these experiments it was noticed that the level of F_0 declined, despite the fact that samples were always measured at the same concentration of chlorophyll and phycobiliprotein. It is noted in this regard that the HA treatment did not discernibly alter the sample pigment composition (not shown). Furthermore, the decline in F_0 correlated with development of O_2 evolution activity during photoactivation: Figure 2B shows that the reciprocal of F_0 was proportional to restoration of oxygen evolution during photoactivation; however, as discussed below, the rate of F_0 decline was slower than the rate of photoactivation.

To better explore these results, the fluorescence properties of cells undergoing photoactivation were monitored in real time (Figures 3). For this experiment, HA-extracted cells were photoactivated directly in the fluorometer using ultrabright red LEDs as an actinic source, instead of photoactivating using a xenon flash lamp in a separate vessel prior to measuring fluorescence as for Figures 1 and 2. In addition to using the weak red measuring flash (RMF, $\lambda_{max} = 617$ nm), as had been utilized for the experiments of Figures 1 and 2, the experiment was also conducted using blue measuring flash (BMF, $\lambda_{max} = 455$ nm). It was noticed during these experiments that HA-extraction produced an approximately 20% increase in the value of F_0 when assayed with RMF, whereas no such increase in fluorescence was observed when yields were probed using BMF, as discussed below. Photoactivation was promoted by application of 1000 flashes, and changes in fluorescence yield were recorded using RMF or BMF. Changes in fluorescence yield during photoactivation measured using RMF (panel A) exhibited a

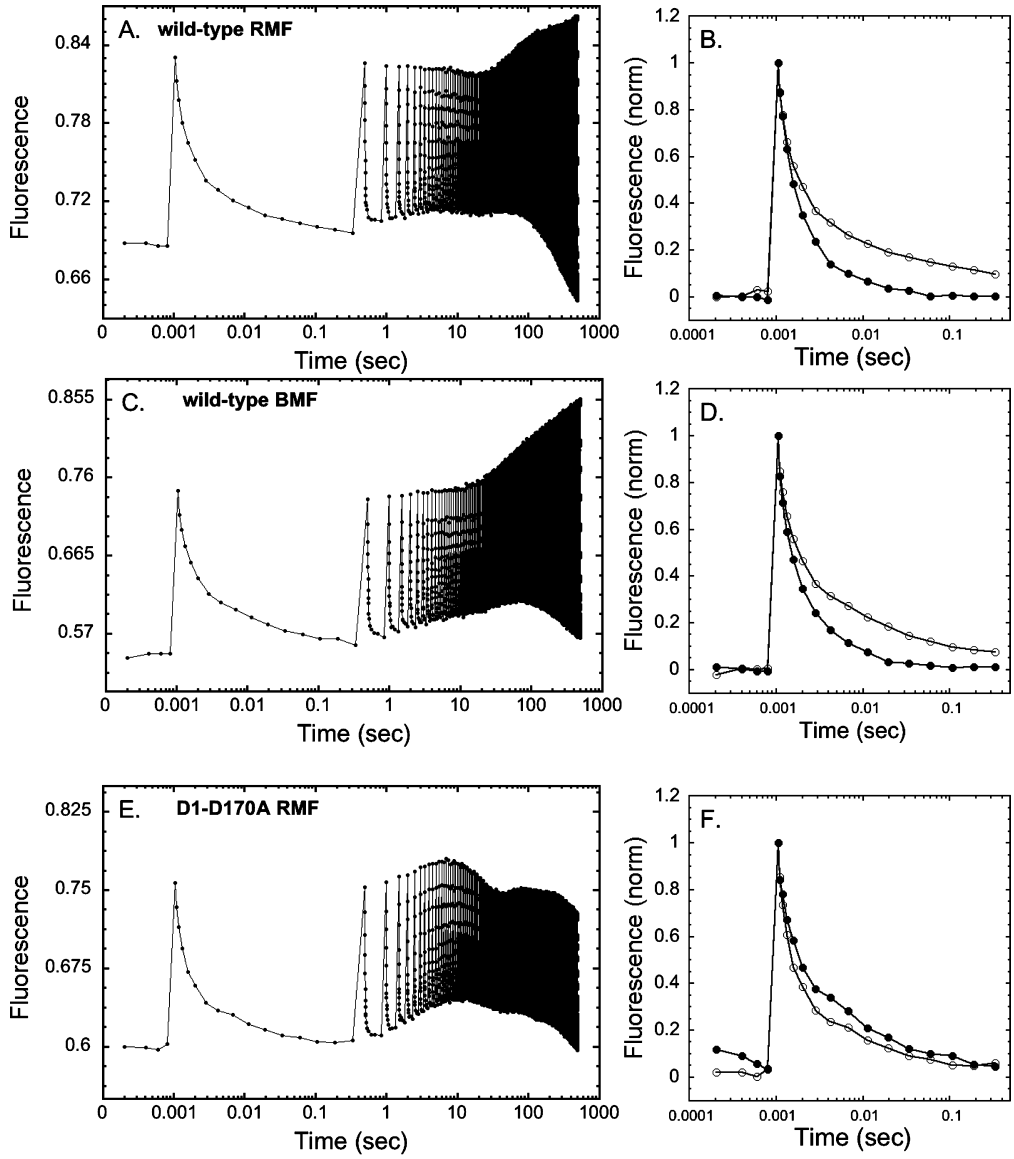

FIGURE 3: Changes of fluorescence yield during photoactivation using either red or blue measuring flashes (RMF or BMF). Photoactivation promoted by application of 1000 flashes at 0.5 s intervals (500 s) and changes in fluorescence yield are recorded using RMF or BMF. Left panels: Fluorescence measured RMF for hydroxylamine-extracted wild-type cells (panel A) or blue measuring flashes (BMF) (panel C), and in a PSII mutant, D1-D170A, that assembles wild-type levels of PSII proteins, but are unable to assemble a Mn_4-Ca (panel E). Right panels: Normalized individual traces of the relaxation of fluorescence yield for the first (open symbols) and last (closed symbols) actinic flashes of the corresponding 1000 flash photoactivation sequences shown to the left.

characteristic pattern where the minimal level of fluorescence (F_0') progressively declined during the course of photoactivation, although never reached the original pre-extraction level F_0 during the course of the flashing. In contrast, the changes in fluorescence yield monitored using BMF (panel C) did not exhibit a decline in F_0' and the initial and final levels of F_0' were nearly identical to the original pre-extraction level F_0 measured with BMF. The right panels of Figure 3 depict normalized individual traces of the relaxation of fluorescence yield for the first (open symbols) and last (filled symbols) actinic flashes of the corresponding 1000 flash photoactivation sequences shown to the left in Figure 3. The kinetics of relaxation of fluorescence yield for the first and last flashes were very similar for the samples probed either RMF (Figure 3B) or BMF (Figure 3D), and both samples exhibited an acceleration of the decay of fluorescence in the photoactivated state of the sample (filled symbols) in comparison to the initial, un-photoactivated state (open symbols). This corresponds to the conversion of the midpoint potential of Q_A^-/Q_A to more negative values during the course of photoactivation, with the consequent increase in the rate of forward electron transfer from Q_A^- to Q_B observed previously (*7, 34*).

To determine whether the decline in F_0' monitored with RMF is dependent upon the ability to assemble an active Mn_4-Ca, a PSII mutant unable to assemble an Mn_4-Ca was subjected to a similar HA-extraction conditions and given photoactivation flash sequence while fluorescence yields probed with RMF. This mutant, D1-D170A, assembles wild-type levels of PSII reaction centers, but has a defect in the high affinity Mn-binding site and has been demonstrated to be defective in photooxidizing Mn^{2+} and thereby is incapable assembling an Mn_4-Ca (*23–26*). Like the wild-type photoactivated with BMF, the nonassembling mutant did not exhibit a decline in F_0'. Furthermore, the mutant did not exhibit a progressive increase in maximal level of variable

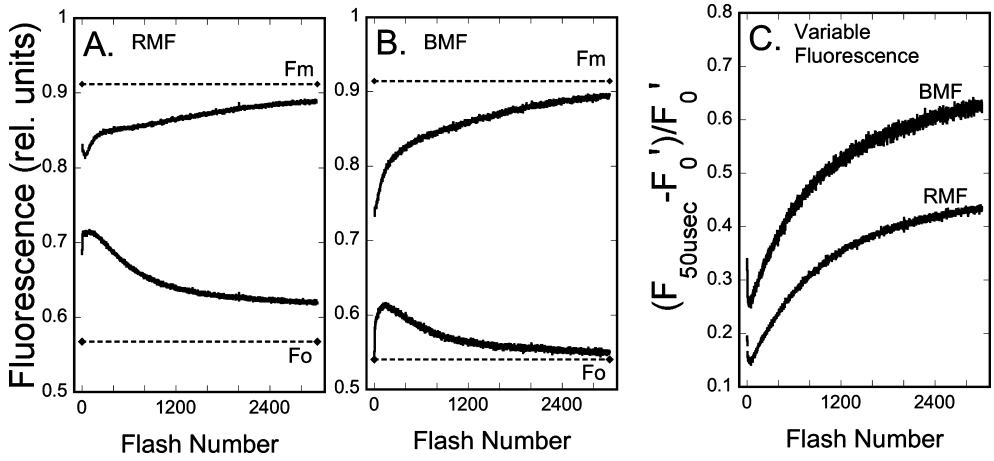

FIGURE 4: Changes of $F_{m,50\mu s}$ and F_0' occurring during flash photoactivation. Sequences of photoactivating flashes were given with a uniform interval of 0.5 s to HA-extracted WT cells. Fluorescence was measured with red measuring flash (panel A) or blue measuring flash (panel B) using the fluorometer (FL 3000, PSI, Czech). Decrease of F_0 was observed during photoactivation using red measuring flashes (RMF). But a decrease of F_0 was not observed using blue measuring flashes (BMF). F_m rapidly increased around flashes during photoactivation and then gradually increased up to 3000 flashes. These experiments were performed at least four times, and representative traces are shown along with the F_m and F_0 values (dotted horizontal lines) of the corresponding cells prior to hydroxylamine treatment. Panel C: The traces of the development of variable fluorescence calculated from the arrays of fluorescence values immediately prior to and after each photoactivating actinic flash (F_0' and $F_{50\mu s}$, respectively) according to the equation $F_v = (F_{50\mu s} - F_0')/F_0'$.

fluorescence as observed during photoactivation of the wild-type observed with either RMF or BMF, which is consistent with the mutant being incapable for forming an active WOC. These results indicate that the decline in F_0' observed using RMF, but not BMF, minimally depends upon the ability to photooxidize Mn^{2+} at the high affinity site of the WOC.

It was also noticed that the F_0 level increased during the ~100 flashes and then declined during the remainder of the photoactivation sequence. This transient change in F_0 is most clearly discerned when the photoactivation is probed with BMF, whereas the transient seems to be superimposed upon the overall decline in F_0 observed with RMF. As discussed in the next section, this transient may reflect an interplay of events involving secondary electron donors capable of reducing P_{680}^+ and changes in the acceptor side that accompany photoactivation.

Figure 4 shows photoactivation experiments recording changes in fluorescence as a function of flash number over the course of a 3000 flash photoactivation experiment, to better visualize the changing minimal fluorescence yields over a longer period of photoactivation. Only the changing values of maximal and minimal fluorescence, $F_{50\mu s}$ and F_0', were recorded. The maximal fluorescence, $F_{50\mu s}$, values correspond to the fluorescence yields observed 50 μs after each photoactivating flash, and F_0' is the fluorescence level immediately prior to these flashes. It can be seen that in both RMF (Figure 4A) and BMF (Figure 4B), F_0' rises during the first 200 photoactivating flashes and then declines. The initial rise in F_0' likely corresponds to the relatively slow transfer of electrons from Q_A^- to Q_B due to the more positive midpoint potential of Q_A^-/Q_A in the absence of an assembled Mn_4-Ca (*7, 34*) as note above. This slower forward electron transfer combined with the reduction of P_{680}^+ and $Y_Z^\cdot$ by Mn^{2+} or secondary donors blocking back-reaction would tend to cause the accumulation of the fluorescent P_{680}-Q_A^- state disallowing oxidation of Q_A^- via back-reaction. These factors prevent complete relaxation of fluorescence due to Q_A^- reoxidation before the subsequent photoactivating actinic flash and thereby the initial phase exhibits a progressive increase in F_0'. This upward trend is probably balanced by processes that tend to quench fluorescence: (1) loss of Q_A^- by transfer, albeit slower, of electrons from Q_A^- to Q_B and (2) depletion of secondary donors, which would result in the accumulation of P_{680}^+, which also acts as a quencher (*32, 33*). This initial phase is followed by a decline in F_0' which is likely due to the conversion of the midpoint potential of Q_A^-/Q_A to the more negative value associated with active PSII as the light-driven assembly of Mn_4-Ca progresses restoring a configuration of redox cofactors permitting the rapid reoxidation of Q_A^- and the efficient rereduction of the oxidized primary donor, P_{680}^+. With RMF (Figure 4A), the F_0' declined below the initial value as noted above, whereas the BMF trace (Figure 4B) declined asymptotically back to the initial value of F_0', which coincides with the F_0 measured in the corresponding sample prior to extraction with HA.

Figure 4C depicts the development of variable fluorescence measured in real time with RMF and BMF. The traces were calculated from the traces in the adjacent panels to the left according to the equation $F_v = (F_{50\mu s} - F_0')/F_0'$. A higher final F_v is obtained using BMF as compared with RMF since the latter has a higher F_0 upon HA-extraction and does not return to the pre-extraction levels during the course of the 3000 flashes. Both traces are similar, however, in the rate of increase as a function of flash number and in having a rapid initial decline in the first 40 flashes. A reasonable assignment for this rapid initial decline phase is the depletion of immediately available secondary electron donors and the resulting accumulation of the quencher P_{680}^+, the level of which gradually declines as photoactivation progresses and allows the formation of the fluorescent P_{680}-Q_A^- state.

The observation that F_0 was dramatically increased by HA-extraction and progressively declined during photoactivation when RMF, but not when BMF was used to probe fluorescence, is suggestive of changes in the coupling of the phycobilisome to the PSII reaction center (RC). Since the RMF light probe mainly excites bilin pigments of the light-harvesting phycobilisome (PBS), whereas BMF light excites

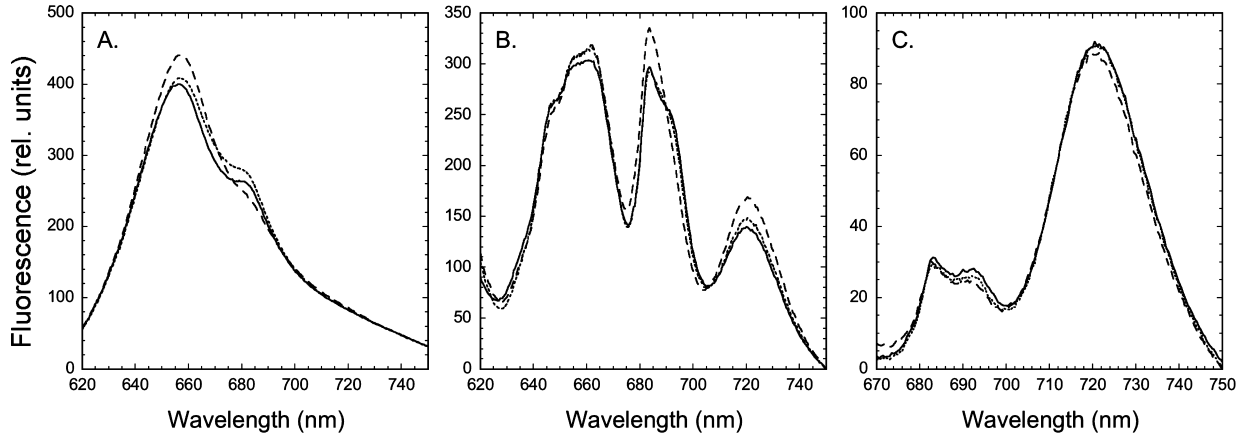

FIGURE 5: Fluorescence emission spectra of control, HA-extracted and photoactivated cells. To photoactivate HA-extracted cells, 1000 flashes were given with a uniform interval of 0.5 s to HA-extracted WT cells. Fluorescence emission spectra of control (solid line), the HA-extracted (dashed line) and the photoactivated cells (dotted line). Panel A: Room temperature emission spectra with phycobilin excitation (600 nm). Panels B and C: 77 K emission spectra of control and the HA-extracted cells and the photoactivated cells at exciting phycobilins at 600 nm (B) and chlorophyll at 435 nm (C) excitation. The emission spectra are presented in un-normalized form in a manner that approximates relative emission intensities as described in the Materials and Methods.

principally chlorophyll, the changes in F_0 observed with RMF appear to reflect changes in the coupling of PBS to the PSII RC. Since a precedent exists for alterations in PBS coupling due to mutational loss of the PsbU of the *Synechocystis* WOC (*35*), a reversible transmembrane perturbation of coupling dependent upon the assembly state of the Mn_4-Ca is a plausible hypothesis. To test this, energy transfer from PBS to PSII RC was investigated using room temperature and low temperature fluorescence spectroscopy. The room temperature emission fluorescence spectrum due to excitation centered at 600 nm yielded fluorescence peaks at 657 nm (F655) and 681 nm (F680) (Figure 5A). The F655 peak originates from phycocyanin (PC) and allophycocyanin (APC), whereas F680 emissions are ascribed to PSII reaction center chlorophylls (*12, 23*). Consistent with the uncoupling of the PBS from PSII, the fluorescence due to PC and APC is increased relative to unextracted control cells (solid line) upon HA-extraction (long-dashed line), and then lowered upon photoactivation (dotted line). In addition to the reversible changes, it is apparent is that the HA-extraction causes some damage to the phycobilisome fluorescence characteristics since the higher fluorescence levels after HA-extraction are not entirely reversed. Also consistent with PBS uncoupling from the reaction center, it was observed that the F680 emission was severely diminished when Mn was removed by HA and then restored after photoactivation. This emission corresponds to reaction center emission that increases as samples approach the F_m state (*36*). Apparently, the excitation intensity of the fluorescence spectrophotometer was high enough to drive a significant accumulation of Q_A^- in samples with a function Mn_4-Ca, whereas this emission was minimal under virtually identical data acquisition conditions for the HA-extracted sample.

The 77 K fluorescence emission spectra had three peaks at 685 nm, 695 nm, and 720 nm (F685, F695, and F720, respectively), when 435 nm light was used to preferentially excite Chl (Figure 5C). F685 and F695 originate from PSII, and PSI is the primary source of emission F720. The 77 K emission spectra were similar in the control cells and the HA-extracted cells when 435 nm light was used to excite Chl (Figure 5C). This indicates that the integrity within the PSII core complex has been maintained such that coupling of Chl to the reaction center pigments responsible for the F685 and F695 emissions is normal and that the relative amounts of these emitters in the photosynthetic membranes are not discernibly perturbed by the HA-extraction. Furthermore, it suggests that the samples, which were dark-adapted >10 min, are all in the same excitation energy distribution state, presumably State 2, since changes in the amplitudes of theses emissions are observed upon state changes in *Synechocystis* (*37*).

In contrast to Chl excitation, a significant change was observed in the emission spectra upon excitation with 600 nm light, which preferentially excites phycobilins (Figure 5B). The F695 shoulder disappeared in the HA-extracted cells and was recovered after the cells were subjected to photoactivation (Figure 5B). F695 is associated with PSII emission, whereas F685 can be ascribed to emission from both PSII and the terminal emitter of the phycobilisome. There was also an increase in F685, which is likely the result of increased emissions from the terminal emitter of the phycobilisome due to decoupling from the reaction center. The changes of F695 and F685 in HA-extracted samples are thus likely a result of decreased efficiency of energy transfer from PBS to Chl a of PSII RC. Furthermore, the recovery of the diminished peaks after photoactivation treatment reflects restoration of energy transfer from PBS to Chl a of PSII RC. These results suggest that removal of Mn ions from WOC induces the decoupling of PBS from the PSII reaction center and that coupling is restored under conditions that promote the reassembly of the Mn_4-Ca. It is also apparent that HA-extracted samples exhibited a reversible increase in PSI emission (F720). One possible explanation is that the PBS that uncouple from PSII become energetically linked to PSI as discussed below. The HA-extraction appears to result in some damage to the phycobilisome fluorescence characteristics evidenced by the nonreversible increase in the level of fluorescence in the 650 nm region.

DISCUSSION

During the course of probing changes in the fluorescence yield relaxation kinetics that accompany photoactivation, it was observed that the basal yield of fluorescence, F_0,

generally increased upon the extraction of cells with HA, a reductant used remove Mn from the PSII H_2O-oxidation complex in preparation for studying the light-driven reassembly (photoactivation) of the Mn_4-Ca. Interestingly, this increase in F_0 was partially reversed by photoactivation of the sample (Figures 3 and 4). Since this reversible increase in basal fluorescence was only observed when probed with red measuring flashes, but not when blue measuring flashes were employed to probe fluorescence yield, it was hypothesized that the destruction of the Mn_4-Ca caused a reversible alteration in the excitation energy coupling of the phycobilisome. This was evaluated by examining the changes in the fluorescence emission properties due to HA-extraction and photoactivation of HA-extracted samples (Figure 5). Energy transfer from phycobilin to PSII chlorophyll is uncoupled by HA-extraction as indicated by the loss of the F695 emission that is normally seen with the excitation of phycobilins. The F695 emission emanates from chlorophyll(s) of the CP47 protein, which function as proximal antennae for the PSII reaction center. This chlorophyll is normally coupled to the terminal phycobilisome emitter, and the disturbance of this coupling diminishes the extent of energy transfer from the phycobilisome to PSII as evidenced by decreased of emission from F695 (*29*). Since this emission is lost only when phycobilisome excitation is used, but is still present when chlorophyll excitation is used, it can be concluded that the HA-extraction affects phycobilisome coupling to PSII chlorophyll but does not perturb the PSII reaction center chlorophylls *per se*. Therefore, the loss of F695 after HA-extraction is due to impaired excitation energy transfer from phycobilisome to PSII. At the same time, the loss of F695 is also accompanied by an increase in PSI (F720) emission. This is interpreted as being due to stronger energetic coupling between the PBS and PSI upon uncoupling the PBS−PSII interaction. This is consistent with the concept that the PBS is a rather flexible, nonspecific antenna wherein photosystem complex essentially competes for binding to the PBS complex.

Heat or high light also impairs excitation energy transfer from phycobilisome to Chl. Disruption of excitation energy transfer from PBS to Chl is observed in heat-treated *Synechocystis* cells, which also display the specific loss of the F695 low temperature emission and, like the present results, also exhibited a decline of F680 shoulder of the room temperature emission spectrum arising from phycobilin excitation (*38*). Certain mutations in cyanobacteria also appear to affect the extent of the F695 emission of PSII and are ascribed to altered phycobilisome coupling. Disruption of the ORF slr0947 (also known as Ycf27 and RpaB) of *Synechocystis*, which is an OmpR-type transcriptional response regulator having a DNA-binding domain, eliminated F695 produced by phycobilisome excitation. This, together with the observation that the F695 emission was still present upon chlorophyll excitation, was taken to indicate that the disruption of ORF slr0947 decoupled the phycobilisome from the PSII reaction center chlorophylls (*29*). The mechanism by which a transcriptional response regulator affects energy transfer from phycobilisomes to photosystems remains unknown; however, ORF slr0947 was recently assigned a function in modulating the expression of high light responsive *hli* genes and perhaps the *psbA* gene encoding the rapidly metabolized D1 protein of PSII (*39, 40*).

In the context of the present results, perhaps the most relevant cyanobacterial mutant that affects phycobilisome coupling is the ΔPsbU mutation. A large increase in the low temperature F685 emission, without a corresponding increase in the F695 emission, was observed in ΔPsbU mutant cells. The mutant also exhibited an elevated F_0 compared to the wild-type and combined with the results of other assays allowed the conclusion that the genetic loss of the PSII PsbU protein caused a decoupling of the phycobilisome to the reaction center (*36*). This result is surprising since the PsbU protein is located on the lumenal side of the membrane where it is involved in maintaining structural stability and activity of the WOC (*36*). This observation suggests that structural alterations on the lumenal side of the membrane, where PsbU is situated, can be allosterically transmitted to the other side of the membrane in a manner that strongly affects the coupling of the phycobilisome to the PSII reaction center chlorophylls. It is probably worth mentioning that the differences in the relative intensities of the different emissions seen in the spectra of that study compared to the spectra shown here may be due, at least in part, to the rather different cell growth conditions employed in the two studies (*36*). Cells in our experiments were grown at considerably higher light intensities (80 versus 30 μmol of photons m^{-2} s^{-1}) and gas conditions (bubbling with air enriched with CO_2 versus growth under ambient atmosphere).

The observation that the uncoupling of the phycobilisome from PSII was reversible by conditions promoting the reassembly of the Mn_4-Ca cluster is consistent with the argument that the assembly state of the Mn_4-Ca cluster modulates phycobilisome coupling, as opposed to the HA treatment having an independent effect on phycobilisome coupling that occurs in parallel with the extraction of PSII Mn. If this were the case, then the light flashing associated with the photoactivation treatment would also have cause phycobilisome reassociation occurring in parallel with Mn_4-Ca assembly. Likewise, the importance of Mn_4-Ca formation in promoting strong phycobilisome coupling is consistent with the finding that the flash-induced decline in F_0 depends upon the ability to photooxidize Mn^{2+} at the high affinity site of the WOC since the high affinity site mutant D1-D170A did not display the decrease in F_0 when subjected to the same photoactivation protocol. It is reasonable that formation of the Mn_4-Ca induces an allosteric change in the conformation of the electron acceptor side of the PSII complex allowing stronger excitonic coupling between reaction center chlorophylls and the terminal emitter(s) of the phycobilisome. A structural coupling between the donor and acceptor side accompanying photoactivation is already well-documented and includes alterations in the distribution of redox forms of cytochrome b_{559} and a downshift in the midpoint potential of Q_A/Q_A^-, both of which may have a photoprotective function (*7, 12, 34*). Nevertheless, these results by no means exclude alternative interpretations. For example, it remains possible that sustained electron transport capacity, absent in D1-D170A and gradually developed during the course of photoactivation, is required for strong phycobilisome coupling. Still, the interpretation that Mn_4-Ca assembly allosterically regulates phycobilisome association is attractive given the facts regarding donor and acceptor side coupling during photoactivation (*7, 12, 34*), on the one

hand, and the finding that the ΔPsbU mutation strongly affects phycobilisome coupling, on the other (*36*).

Overall, the results may offer some physiological insight into the complex mechanisms associated with the operation and biogenesis of photosynthetic membranes. Light intensities that are optimum for driving photosynthesis are supersaturating for the process of photoactivation due to the kinetic features of Mn_4-Ca cluster assembly (*15, 17, 19–21*). PSII centers undergoing photoactivation are, therefore, potentially at a higher risk of incurring photoactivation due to the fact that PSII is highly prone to photodamage in the absence of an intact Mn_4-Ca cluster (*7–14*). Cells of oxygenic phototrophs exposed to typical environmental conditions are likely to have a mixed population of PSII centers. This will include fractions that are either in the process of *de novo* PSII synthesis or in the process of repair by synthesis of a replacement D1 protein in response to photodamage (*35, 41*). Both of these situations require photoactivation to form an active WOC, and the size of their light harvesting antennae, typically optimized for driving high turnover reaction center operation, energetic coupling of the antennae to partially assembled PSII could be destructive. Therefore, the issue of oversaturation of the natural photoactivation process is likely of general physiological significance for oxygenic phototrophs. Consequently, a mechanism regulating the energetic coupling of reaction centers to light-harvesting antennae, such that strong coupling is deferred to the end of the PSII assembly process, would provide a functional solution for the avoidance of photodamage to centers that have yet to finish the assembly of a functional WOC.

ACKNOWLEDGMENT

The authors wish to express thanks to Professor Conrad Mullineaux for helpful discussions. The authors also wish to express gratitude to Professor Rick Debus for access to the *Synechocystis* sp. PCC6803 D1-D170A strain.

REFERENCES

1. Ono, T. (2001) Metallo-radical hypothesis for photoassembly of $(Mn)_4$ cluster of photosynthetic oxygen evolving complex. *Biochim. Biophys. Acta 1503*, 40–51.
2. Burnap, R. L. (2004) D1 protein processing and Mn cluster assembly in light of the emerging photosystem II structure. *Phys. Chem. Chem. Phys. 6*, 4803–4809.
3. Ferreira, K. N., Iverson, T. M., Maghlaoui, K., Barber, J., and Iwata, S. (2004) Architecture of the photosynthetic oxygen-evolving center. *Science 303*, 1831–1838.
4. Kamiya, N., and Shen, J. R. (2003) Crystal structure of oxygen-evolving photosystem II from Thermosynechococcus vulcanus at 3.7 A resolution. *Proc. Natl. Acad. Sci. U.S.A. 100*, 98–103.
5. Loll, B., Kern, J., Saenger, W., Zouni, A., and Biesiadka, J. (2005) Towards complete cofactor arrangement in the 3.0 A resolution structure of photosystem II. *Nature 438*, 1040–1044.
6. Zouni, A., Witt, H. T., Kern, J., Fromme, P., Krauss, N., Saenger, W., and Orth, P. (2001) Crystal structure of photosystem II from Synechococcus elongatus at 3.8 Å resolution. *Nature 409*, 739–743.
7. Rova, M., Mamedov, F., Magnuson, A., Fredriksson, P. O., and Styring, S. (1998) Coupled activation of the donor and the acceptor side of photosystem II during photoactivation of the oxygen evolving cluster. *Biochemistry 37*, 11039–11045.
8. Buser, C. A., Thompson, L. K., Diner, B. A., and Brudvig, G. W. (1990) Electron transfer reactions in manganese depleted photosystem II. *Biochemistry 29*, 8977–8985.
9. Buser, C. A., Diner, B. A., and Brudvig, G. W. (1992) Photooxidation of cytochrome b_{559} in oxygen evolving photosystem II. *Biochemistry 31*, 11449–11459.
10. Poulson, M., Samson, G., and Whitmarsh, J. (1995) Evidence that cytochrome b_{559} protects photosystem II against photoinhibition. *Biochemistry 34*, 10932–10938.
11. Allakhverdiev, S. I., Klimov, V. V., and Carpentier, R. (1997) Evidence for the involvement of cyclic electron transport in the protection of photosystem II against photoinhibition: influence of a new phenolic compound. *Biochemistry 36*, 4149–4154.
12. Magnuson, A., Rova, M., Mamedov, F., Fredriksson, P. O., and Styring, S. (1999) The role of cytochrome b_{559} and tyrosineD in protection against photoinhibition during in vivo photoactivation of photosystem II. *Biochim. Biophys. Acta 1411*, 180–191.
13. Mizusawa, N., Yamashita, T., and Miyao, M. (1999) Restoration of the high-potential form of cytochrome b_{559} of photosystem II occurs via a two-step mechanism under illumination in the presence of manganese ions. *Biochim. Biophys. Acta 1410*, 273–286.
14. Bondarava, N., De Pascalis, L., Al-Babili, S., Goussias, C., Golecki, J. R., Beyer, P., Bock, R., and Krieger-Liszkay, A. (2003) Evidence that cytochrome b_{559} mediates the oxidation of reduced plastoquinone in the dark. *J. Biol. Chem. 278*, 13554–13560.
15. Cheniae, G. M., and Martin, I. F. (1971) Photoactivation of the manganese catalyst of O2 evolution. I. Biochemical and kinetic aspects. *Biochim. Biophys. Acta 253*, 167–181.
16. Hwang, H. J., McLain, A., Debus, R. J., and Burnap, R. L. (2007) Photoassembly of the Manganese Cluster in Mutants Perturbed in the High Affinity Mn-Binding Site of the H_2O-Oxidation Complex of Photosystem II. *Biochemistry 46*, 13648–13657.
17. Tamura, N., and Cheniae, G. (1987) Photoactivation of the water-oxidizing complex in photosystem II membranes depleted of Mn and extrinsic proteins. I. Biochemical and kinetic characterization. *Biochim. Biophys. Acta 890*, 179–194.
18. Zaltsman, L., Ananyev, G. M., Bruntrager, E., and Dismukes, G. C. (1997) Quantitative kinetic model for photoassembly of the photosynthetic water oxidase from its inorganic constituents: requirements for manganese and calcium in the kinetically resolved steps. *Biochemistry 36*, 8914–8922.
19. Ananyev, G. M., and Dismukes, G. C. (1996) High resolution kinetic studies of the reassembly of the tetra manganese cluster of photosynthetic water oxidation: proton equilibrium, cations, and electrostatics. *Biochemistry 35*, 14608–14617.
20. Miller, A. F., and Brudvig, G. W. (1989) Manganese and Calcium Requirements for Reconstitution of Oxygen-Evolution Activity in Manganese-Depleted Photosystem-II Membranes. *Biochemistry 28*, 8181–8190.
21. Burnap, R. L., Qian, M., and Pierce, C. (1996) The manganese-stabilizing protein (MSP) of photosystem II modifies the in vivo deactivation and photoactivation kinetics of the H_2O-oxidation complex in Synechocystis sp. PCC6803. *Biochemistry 35*, 874–882.
22. Williams, J. G. K. (1988) Construction of specific mutations in Photosystem II photosynthetic reaction center by genetic engineering methods in Synechocystis 6803. *Methods Enzymol. 167*, 766–778.
23. Chu, H.-A., Nguyen, A. P., and Debus, R. A. (1994) Site-directed mutagenesis of photosynthetic oxygen evolution: Instability or inefficient assembly of the manganese cluster in vivo. *Biochemistry 33*, 6137–6149.
24. Boerner, R. J., Nguyen, A. P., Barry, B. A., and Debus, R. J. (1992) Evidence from directed mutagenesis that aspartate 170 of the D1 polypeptide influences the assembly and-or stability of the manganese cluster in the photosynthetic water-splitting complex. *Biochemistry 31*, 6660–6672.
25. Komenda, J., Hassan, H. A. G., Diner, B. A., Debus, R. J., Barber, J., and Nixon, P. J. (2000) Degradation of the Photosystem II D1 and D2 proteins in different strains of the cyanobacterium Synechocystis PCC 6803 varying with respect to the type and level of psbA transcript. *Plant Mol. Biol. 42*, 635–645.
26. Nixon, P. J., and Diner, B. A. (1992) Aspartate 170 of the photosystem II reaction center polypeptide D1 is involved in the assembly of the oxygen evolving manganese cluster. *Biochemistry 31*, 942–948.
27. Cheniae, G. M., and Martin, I. F. (1972) Effects of hydroxylamine on photosystem II. II Photoreversal of the NH_2OH destruction of O_2 evolution. *Plant Physiol. 50*, 87–94.
28. Hwang, H. J., and Burnap, R. L. (2005) Multiflash experiments reveal a new kinetic phase of photosystem II manganese cluster assembly in Synechocystis sp PCC6803 in vivo. *Biochemistry 44*, 9766–9774.
29. Kramer, D. M., Robinson, H. R., and Crofts, A. R. (1990) A portable multi-flash kinetic fluorimeter for measurement of donor

and acceptor reactions of photosystem 2 in leaves of intact plants under field conditions. *Photosynth. Res. 26*, 181–194.
30. Trtilek, M., Kramer, D. M., Koblizek, M., and Nedbal, L. (1997) Dual-modulation LED kinetic fluorometer. *J. Lumin. 724*, 597–599.
31. Allakhverdiev, S. I., Karacan, M. S., Somer, G., Karacan, N., Khan, E. M., Rane, S. Y., Padhye, S., Klimov, V. V., and Renger, G. (1994) Reconstitution of the water oxidizing complex in manganese depleted photosystem II complexes by using synthetic binuclear manganese complexes. *Biochemistry 33*, 12210–12214.
32. Mauzerall, D. (1972) Light-Induced Fluorescence Changes in Chlorella, and Primary Photoreactions for Production of Oxygen. *Proc. Natl. Acad. Sci. U.S.A. 69*, 1358.
33. Sonneveld, A., Rademaker, H., and Duysens, L. N. M. (1979) Chlorophyll-a Fluorescence as a Monitor of Nanosecond Reduction of the Photo-Oxidized Primary Donor P-680$^+$ of Photosystem-Ii. *Biochim. Biophys. Acta 548*, 536–551.
34. Johnson, G. N., Rutherford, A. W., and Krieger, A. (1995) A change in the midpoint potential of the quinone Q_A in photosystem II associated with photoactivation of oxygen evolution. *Biochim. Biophys. Acta 1229*, 202–207.
35. Veerman, J., McConnell, M. D., Vasil'ev, S., Mamedov, F., Styring, S., and Bruce, D. (2007) Functional heterogeneity of photosystem II in domain specific regions of the thylakoid membrane of spinach (Spinacia oleracea L.). *Biochemistry 46*, 3443–3453.
36. Veerman, J., Bentley, F. K., Eaton-Rye, J. J., Mullineaux, C. W., Vasil'ev, S., and Bruce, D. (2005) The PsbU Subunit of Photosystem II Stabilizes Energy Transfer and Primary Photochemistry in the Phycobilisome-Photosystem II Assembly of Synechocystis sp. PCC 6803. *Biochemistry 44*, 16939–16948.
37. McConnell, M. D., Koop, R., Vasil′ev, S., and Bruce, D. (2002) Regulation of the distribution of chlorophyll and phycobilin-absorbed excitation energy in cyanobacteria. A structure-based model for the light state transition. *Plant Physiol. 130*, 1201–1212.
38. Stoitchkova, K., Zsiros, O., Javorfi, T., Pali, T., Andreeva, A., Gombos, Z., and Garab, G. (2007) Heat- and light-induced reorganizations in the phycobilisome antenna of Synechocystis sp. PCC 6803. Thermo-optic effect. *Biochim. Biophys. Acta 1767*, 750–756.
39. Kappell, A. D., Bhaya, D., and van Waasbergen, L. G. (2006) Negative control of the high light-inducible hliA gene and implications for the activities of the NblS sensor kinase in the cyanobacterium Synechococcus elongatus strain PCC 7942. *Arch. Microbiol. 186*, 403–413.
40. Kappell, A. D., and van Waasbergen, L. G. (2007) The response regulator RpaB binds the high light regulatory 1 sequence upstream of the high-light-inducible hliB gene from the cyanobacterium Synechocystis PCC 6803. *Arch. Microbiol. 187*, 337–342.
41. Melis, A. (1991) Dynamics of photosynthetic membrane composition and function. *Biochim. Biophys. Acta 1058*, 87–106.

BI800568P